ORIGINAL ARTICLE

Determination of [N-13]-ammonia extraction fraction in patients with coronary artery disease by calibration to invasive coronary and fractional flow reserve

Jonathon A. Nye, PhD,[a] Marina Piccinelli, PhD,[a] Doyeon Hwang, MD,[b] C. David Cooke, MSEE,[a] Jin Chul Paeng, MD, PhD,[c] Joo Myung Lee, MD,[d] Sang-Geon Cho, MD, PhD,[e] Russell Folks,[a] Michael Haber, PhD,[f] Hee-Seung Bom, MD,[e] Bon-Kwon Koo, MD, PhD,[b] and Ernest V. Garcia, PhD[a]

[a] Department of Radiology and Imaging Sciences, Emory School of Medicine, Emory University, Atlanta, GA
[b] Department of Internal Medicine and Cardiovascular Center, Seoul National University Hospital, Seoul, Korea
[c] Department of Nuclear Medicine, Seoul National University Hospital, Seoul, Korea
[d] Samsung Medical Center, Heart Vascular Stroke Institute, Seoul, Korea
[e] Department of Nuclear Medicine, Chonnam National University Hospital, Gwangju, Korea
[f] Department of Biostatistics and Bioinformatics, Rollins School of Public Health, Emory University, Atlanta, GA

Background. This study presents a new extraction fraction (EF) model based on physiological measures of invasive coronary flow reserve (CFR) and fractional flow reserve (FFR) in patients with suspected coronary artery disease (CAD) and normal index microcirculatory resistance (IMR). To ascertain the clinical relevance of the new EFs, flow measurements using the newly patient-determined EFs were compared to flow measurements using traditional animal-determined EFs.

Methods. 39 patients were retrospectively selected that included a total of 91 vascular territories with invasive coronary angiography physiological measures. [N-13]-ammonia dynamic rest/adenosine-stress PET imaging was conducted in all patients and absolute myocardial flow was estimated using four published compartmental models. The extraction fraction during hyperemic flow was iteratively estimated by maximizing the agreement between invasive CFR and FFR with the non-invasive analogs myocardial flow reserve (MFR) and relative flow reserve (RFR) at similar physiological states, respectively.

Results. Using the new patient-determined EFs, agreement between CFR vs MFR for Model 1 and 2 was moderate and poor for Model 3 and 4. All models showed moderate agreement for FFR vs RFR. When using published models of animal-determined EFs,

agreement between CFR vs MFR remained moderate for Model 1 and 2, and poor for Model 3 and 4. Similarly, all models showed moderate agreement for FFR vs RFR using animal-determined EF values. None of the observed differences were statistically significant.

Conclusions. Flow measurements using extraction fraction correction for [N-13]-ammonia based on calibration to invasive intracoronary angiography physiological measures in patients with CAD were not discordant from those reported in the literature. Either patient-determined or traditional animal-determined EF correction, when used with the appropriate flow model, yields moderate agreement with invasive measurements of coronary flow reserve and fractional flow reserve. (J Nucl Cardiol 2022;29:2210–9.)

Key Words: Myocardial perfusion imaging · PET flow · [N-13]-ammonia extraction fraction

Abbreviations	
CCC	Concordance correlation coefficient
CFR	Coronary flow reserve
EF	Extraction fraction
FFR	Fractional flow reserve
ICA	Invasive coronary angiography
MFR	Myocardial flow reserve
PS	Permeability and capillary surface area product
RFR	Relative flow reserve
FP	First-pass extraction
RF	Retention fraction

INTRODUCTION

Absolute myocardial blood flow (MBF) using positron emission tomography (PET) under rest and stress conditions is a critical non-invasive clinical tool that addresses many limitations of conventional myocardial perfusion based on relative quantification and normal databases.[1] Evaluation of MBF follows from the application of compartmental analysis techniques to derive an estimate of the tissue unidirectional influx rate, which is related to coronary blood flow.[2] [3] The relationship between radiotracer influx rate and coronary blood flow is based on Fick's principle where the influx rate is equal to the product of coronary blood flow and the difference in radiotracer concentration between the arterial and venous concentrations.[4] Blood flow can be measured during invasive coronary angiography (ICA) on a per vessel basis such as with intracoronary Doppler flow velocity[5,6] and thermodilution techniques.[7,8] Similarly, ICA pressure derived measurements of fractional flow reserve (FFR) represent the ''reference standard'' for assessing the hemodynamic significance of coronary lesions that need revascularization and are now included in revascularization guidelines.[9] Thus, this research is one of our first steps in developing methodology to calibrate MBF PET measurements to harmonize with ICA derived treatment decisions to revascularize coronary lesions.[10,11]

The radiotracer influx rate from PET and coronary blood flow are related by the extraction fraction (EF) which is the difference in arterial and venous concentrations over the arterial concentration. Knowing the extraction fraction, the product of blood flow and extraction fraction is equal to the unidirectional radiotracer influx rate, K_1. If the arterial radiotracer concentration over time is known, K_1 can be estimated using a compartment model and first order kinetic principles. Extraction fraction cannot be measured directly in humans and thus has been estimated from animal models using a combination of unidirectional radiotracers[12,13] to estimate tissue perfusion and microsphere techniques to estimate regional vessel blood flow.[14] Data collected from these experiments are fit to the analytical Renkin-Crone capillary permeability model that equates the radiotracer extraction from blood-to-tissue as a function of coronary blood flow, F, and the permeability and capillary surface area product, PS. When PS is high, or conversely, flow is low, the K_1 estimated from the PET compartment model approximates coronary blood flow.

It is well documented that there are two phases comprising the extraction of radiotracer from blood-to-tissue, the first-pass extraction fraction (FP) and the retention fraction (RF). FP refers to the blood-to-tissue extraction of the radiotracer following its first capillary transit, whereas RF is the net blood-to-tissue extraction of the radiotracer that irreversibly remains in the tissue. Redistribution of radiotracer between the blood and vascular spaces occurs between these two phases but is ignored because the process is fast. Our model of EF described below relies on estimates of K_1 from compartment models therefore it represents the extraction under steady-state conditions where the blood and tissue compartments are in a quasi-equilibrium. In the estimate of blood flow from [N-13]-ammonia perfusion studies, data used to derive FP and RF are based on a canine model[13] with other groups fitting these data to the Renkin-Crone model applying a flow-dependent estimate of PS over a wide range of coronary flows.[15,16] Animal models are highly predictive of human physiology and necessary for estimates of extraction and

blood flow. However, differences exist between human and canine coronary anatomy and physiology.[17–19] With advances in intracoronary measurement techniques, clinical standard of care provides reliable measures of coronary flow reserve (CFR) and FFR, and when conducted in combination with dynamic PET may be used to estimate the blood-to-tissue extraction of the radiotracer in vivo.

We present an in vivo calibration method that uses perfusion from dynamic [N-13]-ammonia PET with invasive CFR and FFR, at similar physiological states during PET, to derive an extraction fraction (EF) in patients with coronary artery disease (CAD). Our goal is to assess whether patient-derived [N-13]-ammonia EFs using modern non-invasive imaging better predicts the ICA measurements of FFR and CFR used to make revascularization treatment decisions compared to animal-derived EFs determined years ago. Patients selected for this analysis have normal index microcirculatory resistance (IMR) as an indicator for the absence of microvascular disease. We present EF results from four different compartment models commonly used in the clinical evaluation of [N-13]ammonia PET MBF and agreement between CFR and FFR with their non-invasive PET analogs myocardial flow reserve (MFR) and relative flow reserve (RFR).

METHODS

Patient Population

This is a retrospective study including 39 patients with CAD based on a positive [N-13]-ammonia PET scan who were then referred for invasive coronary angiography. Of the total 39 patient datasets, 34 were recruited from Seoul National University Hospital, 4 from Chonnam National University Hospital and one from Samsung Medical Center that included [N-13]-ammonia rest and adenosine-stress dynamic PET, CFR and FFR collected between February 2013 and May 2014. The study was approved by the Institutional Review Board of Seoul National University Hospital, Chonnam National University Hospital, Samsung Medical Center and Emory University.

Invasive Physiological Measures

Coronary angiography was performed using clinical procedures previously described by our team.[20,21] Briefly, patients were instructed to cease use of caffeine or xanthine the day before the procedure. A guide wire was advanced into the coronary ostium and standard angiographic views were obtained following intracoronary bolus administration of 100 to 200 μg of nitrates. A

5-F to 7-F catheter guide was advanced into one or more of the three major vessels employing a pressure-temperature sensor (St. Jude Medical, St. Paul, MN) for physiological measurements. The sensor was zeroed and equalized to aortic pressure then placed at the distal segment of the target vessel and intracoronary nitrate was administered prior to measurement. Hyperemia was induced for the estimation of physiological measures by continuous intravenous infusion of 140 μg/kg/min adenosine to sustain a physiological state similar to that during PET measurements. Hyperemic proximal aortic and distal vessel pressures were obtained and FFR was determined by dividing the mean distal arterial pressure by the proximal aortic pressure during hyperemia.

Mean transit time was measured using a thermodilution curve obtained from three separate injections of 4mL room temperature saline. Proximal aortic pressure, distal target vessel arterial pressure and hyperemic mean transit time were measured at sustained hyperemia by intravenous infusion of adenosine through a peripheral or central vein. The presence of pressure drift was checked following pull back of the catheter into the guidewire. CFR was calculated by dividing the resting by the sustained hyperemic mean transit time for one or more of the three major vessel territories, left main artery (LAD), left circumflex artery (LCX), and right coronary artery (RCA). Finally, IMR was estimated as the product of the distal arterial pressure and mean transit time during hyperemia.

PET Myocardial Perfusion Protocol and Processing

Prior to collection of ICA measures (maximum 90 days), [N-13]-ammonia dynamic PET was conducted on a Biograph 40 PET/CT (Siemens Medical Solutions, Erlangen, Germany). Patients were instructed to abstain from caffeinated or xanthine-containing products as well as β-blockers and calcium channel blockers for 24 hours before the procedure. A few minutes prior to the PET scan, a low dose computed tomography scan was collected for the purposes of attenuation and scatter correction. Next, a 10 minute resting dynamic list-mode PET acquisition was started followed immediately by a 370 MBq bolus of [N-13]-ammonia administered via a peripheral radial vein. Hyperemia was induced to sustain a physiological state similar to that during invasive measurements by intravenous infusion of adenosine (140 μg/kg/min) for 3 minutes prior to the start of a 10 minute dynamic list-mode PET acquisition. Adenosine infusion was terminated at 6 min total duration. The time interval between the rest and the stress injections of [N-13]-ammonia was approximately one hour. This delay represents 6 half-lives of N-13 or less than 2%

resting residual activity contaminating the hyperemic study. PET data were binned into 21 frames (12×10 s, 6×30 s, 2×60 s, 1×180 s) and reconstructed with a 3D ordered-subset expectation maximization algorithm (4 iterations, 8 subsets) and all corrections with a matrix size of $168 \times 168 \times 111$ and $1.85 \times 1.85 \times 3$ mm voxels. A 5 mm full width at half maximum Gaussian post-reconstruction filter was applied to all frames.

Dynamic PET data were corrected for motion by registering all time points to a common reference frame as described by Lee et al.[22] Data were reoriented along the short axis and regions of interest were defined on a summed image, consisting of the last half of the acquisition duration, using a region spanning 3mm on either side of the center line of the myocardium from apex to base. The ROI for the arterial input function was defined by placing a 10 mm spherical ROI at the left ventricle base on the frame with the maximum arterial phase concentration. Time-activity curves were extracted from the tissues by applying the ROI mask to all frames.

Four previously reported compartment models used in clinical practice were employed in this work and their implementation and parameters are described in Table 1: Model (1) 2-tissue compartment model that accounts for the conversion of ammonia to glutamine,[2] (2) 1-tissue compartment model with a fixed distribution volume,[16] (3) 1-tissue compartment model assuming irreversible trapping (e.g., retention)[23] and (4) a simplified retention model.[15] Models with iteratively determined free parameters used the Powell multi-dimensional directional set method to minimize the residual summed squares weighted by frame duration. Metabolite correction of the arterial input function was not performed for any model.

Estimation of Extraction Fraction

Calibration of the PET values to the ICA values is done by representing the extraction fraction (EF) during hyperemic flow by an algebraic relationship that equates MBF from rest and stress PET with the invasive CFR and FFR measures,

$$\text{CFR} = \text{MFR} = \frac{\text{MBF}_{\text{stress}}^{\text{targetvessel}}}{\text{MBF}_{\text{rest}}^{\text{targetvessel}}} = \frac{K_{1,\text{stress}}^{\text{targetvessel}} / \text{EF}_{\text{stress}}^{\text{targetvessel}}}{K_{1,\text{rest}}^{\text{targetvessel}} / EF_{\text{rest}}^{\text{targetvessel}}} \tag{1}$$

$$\text{FFR} = \text{RFR} = \frac{\text{MBF}_{\text{stress}}^{\text{targetvessel}}}{\text{MBF}_{\text{stress}}^{\text{normalvessel}}}$$
$$= \frac{K_{1,\text{stress}}^{\text{targetvessel}} / \text{EF}_{\text{stress}}^{\text{targetvessel}}}{K_{1,\text{stress}}^{\text{normalvessel}} / \text{EF}_{\text{stress}}^{\text{normalvessel}}} \tag{2}$$

where MFR is the PET derived myocardial flow reserve equal to the ratio of the myocardial blood flow in the target vessel at stress, $\text{MBF}_{\text{stress}}^{\text{targetvessel}}$, by that at rest in the same target vessel, $\text{MBF}_{\text{rest}}^{\text{targetvessel}}$; $K_{1,\text{stress}}^{\text{targetvessel}}$ and $K_{1,\text{rest}}^{\text{targetvessel}}$ are the PET derived influx rates at stress and rest in the target vessel; $\text{EF}_{\text{stress}}^{\text{targetvessel}}$ and $\text{EF}_{\text{rest}}^{\text{targetvessel}}$ are the extraction fractions in the target vessel at stress and rest; $K_{1,\text{stress}}^{\text{normal vessel}}$ is the highest PET derived influx rate among the three vessel territories in the myocardium; and $\text{EF}_{\text{stress}}^{\text{normalvessel}}$ is the extraction fraction associated with $K_{1,\text{stress}}^{\text{normal vessel}}$.

We assume that $\text{EF}_{\text{rest}}^{\text{targetvessel}} = 1$ at low flow. In addition, we assume that $\text{EF}_{\text{stress}}^{\text{targetvessel}}$ and $\text{EF}_{\text{stress}}^{\text{normalvessel}}$ share the same functional relationship described by the Renkin-Crone extraction fraction equation using a flow-dependent PS,

$$\text{EF} = 1 - e^{-\left(\frac{\text{PS}}{\text{MBF}}\right)} \tag{3}$$

where $PS = a + b \times MBF$. Our proposed *in vivo* calibration model iteratively estimates the constants a and b by maximizing the agreement of Eqs. 1 and 2 using a weighted combination of the concordance correlation coefficient (CCC),

$$\max[(w)\text{CCC}(\text{CFR}, \text{MFR}) + (1 - w)\text{CCC}(\text{FFR}, \text{RFR})] \tag{4}$$

where w is set to 1/3rd. The iterative routine uses the Powell multi-dimensional directional set method and is run for each compartment model.

Finally, we examined the agreement of Eq. 1 and 2 using extraction fraction values published as part of each compartment model implementation by their respective authors. Previously published, animal-derived values of a and b are reported in Table 3 along with their reference. Note that the original description of FP and RF by Schelbert et al.[13] takes on a different functional form than eqn 3 but are numerically identical to those reported by Yoshida et al.[15] and Hutchins et al.[2]

Areas of abnormal and normal perfusion were computed using the methods described by Hwang et al.[21] on the 17-segment model[1]. Briefly, $K_{1,\text{stress}}^{\text{targetvessel}}$ in the territory of abnormal perfusion was computed by averaging the lowest three contiguous segments during hyperemia, excluding the basal segments. The same method was applied for computing $K_{1,\text{stress}}^{\text{normal vessel}}$ in the territory with the highest perfusion during hyperemia. The segments identified during hyperemia were transferred directly to the rest perfusion data for computing $K_{1,\text{rest}}^{\text{targetvessel}}$ and $K_{1,\text{rest}}^{\text{normal vessel}}$.

Table 1. Compartment model descriptions of compartments, fixed and free parameters, acquisition duration used in the model fitting, and references

Parameter	Model 1	Model 2	Model 3	Model 4
Compartments	Tissue and metabolite	Tissue only	Tissue only (retention)	Tissue only (retention)
Free parameters	K_1, k_2, k_3, TBV	K_1, DV, TBV	K_1, S_t, S_b	None
Fixed parameters	None	DV	PV_t	PV_t, S_b, S_t
Minimization algorithm	Powell	Powell	Nelder-Mead	None
Acquisition duration modeled	0 to 10 min	0 to 4min	0 to 10min	0 to 1min (blood phase) 1 to 2 min (tissue phase)
Reference(s)	(2) Configuration 2	(16) Technique 3	(23)	(15)

K_1, unidirectional influx rate constant; k_2, unidirectional efflux rate constant; k_3, tissue to metabolite rate constant; DV, distribution volume (K_1/k_2) ; TBV, total blood volume; PV_t, myocardial tissue partial volume correction factor; S_b, spillover correction factor from blood-to-myocardial tissue; S_t, spillover correction factor from myocardial tissue-to-blood

Statistical Analysis

Continuous variables are presented as mean ± standard deviation. Agreement between CFR vs. MFR and FFR vs RFR for each model was examined with the concordance correlation coefficient (CCC).[24] The CCC ranges from − 1 to 1 and takes into consideration measurement bias not accounted for in ordinary correlations (e.g., Pearson). The Pearson and CCC are related by a bias factor, $0 < C_b \leq 1$, where CCC = Pearson × C_b and C_b is computed from the mean and standard deviation of the two distributions being compared.[24] Therefore, the CCC is generally lower than Pearson but can never be higher. Compared to other agreement measures such as the intraclass correlation coefficient (ICC),[25] the CCC and ICC are nearly identical in their numerical outcome.[26] In the interpretation of the CCC, a value below 0.4 is considered poor; a value of 0.4 to 0.7 is moderate; and a value > 0.7 is good agreement.[27] For each CCC measure, the 95% confidence interval is reported using the z-transform methods described by Lin et al.[24] When comparing CCC between models, differences were considered statistically significant if their 95% confidence intervals did not overlap. No corrections were made for multiple comparisons.

RESULTS

Patient demographics and baseline characteristics are summarized in table 2. In 39 patients, 91 vessel territories had FFR and of those, 37 had corresponding CFR measures and all had IRM measures. Mean and standard deviation (range: min to max) of CFR, FFR, an IMR were 3.85 ± 1.68 (1.3 to 9.9), 0.86 ± 0.13 (0.36 to 1.0), and 14.01 ± 3.85 (8 to 24), respectively. IMR < 25 was used as the cut-off value for microvascular disease as previously described.[28]

Table 3 reports the optimized PS constants determined from our iterative model following maximization of the CCC relationships between the invasive and non-invasive measurements. In addition, we report in table 3 the published PS model constants and agreement between the invasive and non-invasive measurements using EF computed from Eq. 3. Across models, agreement between CFR vs MFR and FFR vs RFR was not statistically different using the optimized patient-derived PS constants for the calculation of EF. When using published animal-derived PS constants for EF, agreement between CFR vs MFR was significantly higher for Model 2 compared to Model 3 and no significant differences existed between FFR vs RFR agreements.

Figure 1 shows the graphical relationship between CFR vs MFR and FFR vs RFR for each model using the optimized patient-derived PS constants from this work reported in Table 3. Points that lie on the line of identity would indicate perfect agreement without bias as described in the CCC measure above. Model 1 and 2 showed moderate agreement in both the CFR vs MFR and FFR vs RFR results. In addition, Model 3 and 4 showed moderate agreement in FFR vs RFR but poor agreement in CFR vs MFR. Figure 2 shows the graphical relationship of the same measures, but using previously published animal-derived PS constants for

Table 2. Patient demographics and baseline characteristics (n = 39 patients)

Age (years)	64 ± 9
Sex (Male)	36 (90%)
Demographics	
Body mass index (kg/m^3)	26 ± 4
Height (cm)	167 ± 7
Weight (kg)	70 ± 8
CAD risk factors	
Family history	4 (10%)
Prior MI	4 (10%)
Hypertension	30 (75%)
Hyperlipidemia	35 (90%)
Diabetes mellitus	12 (30%)
Smoking history	25 (63%)
Medication	
Ace inhibitor	3 (8%)
Aspirin	30 (78%)
Beta-blockers	13 (33%)
Nitrates	4 (10%)
Statins	4 (10%)
Hypertension	25 (63%)
Vessels Examined with FFR (CFR)	
LAD	38 (20)
LCx	26 (3)
RCA	27 (14)

EF reported in Table 3. Agreement in CFR vs MFR was moderate for Model 1 and 2 and poor for Model 3 and 4, respectively. Agreement between FFR vs RFR was moderate in all models.

DISCUSSION

This study presents the first human data to estimate [N-13]-ammonia EF by calibrating PET perfusion measures with invasive measures of CFR and FFR in patients with normal IMR. The main findings of this study are that agreement between CFR vs MFR and FFR vs RFR using a patient-derived model for estimation of PS were not discordant with published animal-derived values. Overall agreement was poor to moderate when comparing CFR vs MFR and moderate when comparing FFR vs RFR.

Previous studies comparing invasive CFR with PET MFR have reported a wide range of agreement. Saraste et al.[29] compared [O-15]-water rest/dipyridamole-stress dynamic PET to CFR derived from transthoracic Doppler echocardiography of the LAD in normal volunteers with no prior CAD history or predictors such as diabetes, hypertension and smoking. Using data from their work (see Table 2 in[29]), we computed a CCC for [O-15]-water PET MBF compared to peak diastolic flow, mean diastolic flow, and velocity time integral of 0.85, 0.92, and 0.51, respectively. Everaars et al.,[30]

Table 3. Optimized PS constants (a, b) and agreement by CCC (95% CI) between CFR vs MFR and FFR vs RFR for all compartment models from this work and using published PS constants.

|	Model 1	Model 2	Model 3	Model 4
(This work) Optimized PS				
Model Constants (a,b)	(1.03, 0.35)	(0.85, 0.35)	(0.58, 0.40)	(0.56, 0.31)
CCC (95% CI)				
CFR vs MFR	0.46 (0.23, 0.69)	0.46 (0.24, 0.69)	0.33 (0.13, 0.52)	0.36 (0.16, 0.55)
FFR vs RFR	0.59 (0.43, 0.76)	0.57 (0.41, 0.73)	0.69 (0.51, 0.87)	0.62 (0.44, 0.78)
Published PS Model Constants				
(a, b)	(1.08, 0.234)	(1.08, 0.234)	(2.34, 0)	(1.34, 0.48)
Reference	(13)	(13, 33)	(23)	(15)
CCC (95% CI)				
CFR vs MFR	0.42 (0.19, 0.66)	0.48 (0.24, 0.73)	0.18 (0.06, 0.29)	0.12 (0.04, 0.21)
FFR vs RFR	0.54 (0.39, 0.70)	0.49 (0.35, 0.64)	0.48 (0.32, 0.63)	0.60 (0.43, 0.77)

CCC, concordance correlation coefficient
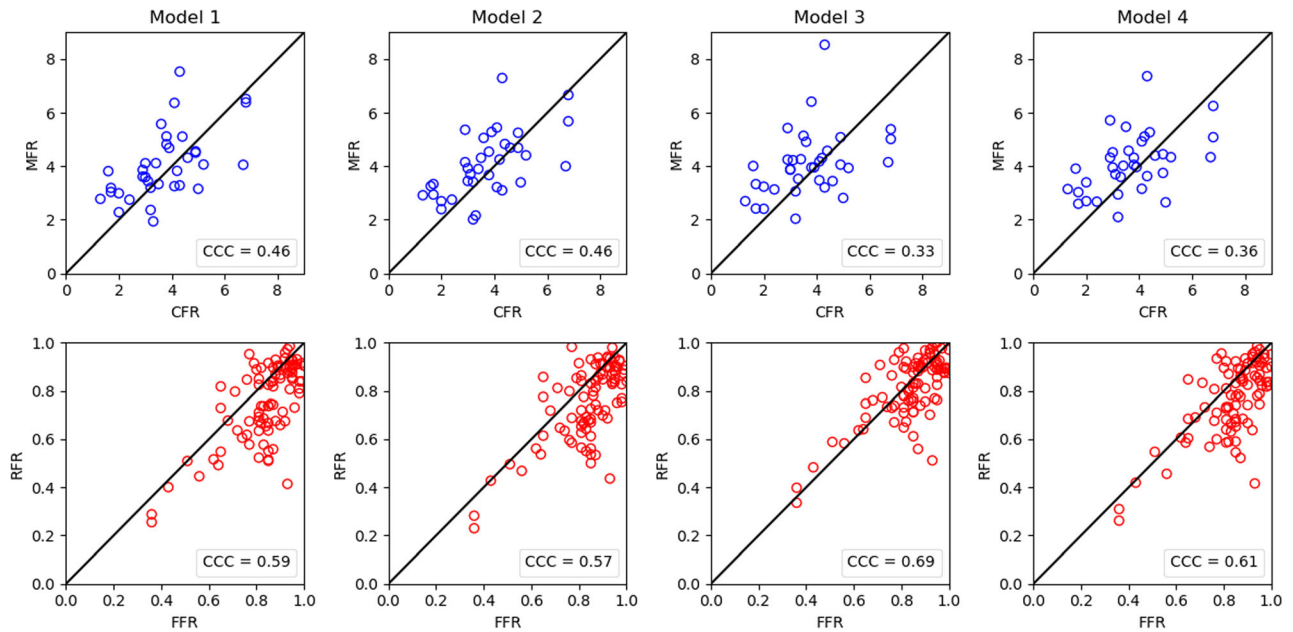
Figure 1. Plots of MFR vs CFR agreement (top row, n = 37) and of RFR vs FFR agreement (bottom row, n = 91) for each compartment model using the proposed optimization model and EF computed from eqn 3 and optimized PS constants from this work reported in Table 3. Note that RFR vs FFR moderate agreement almost reaches good agreement for model 3 (CCC ≥ .7). (PS = the permeability and capillary surface area product; CCC = Concordance correlation coefficient).
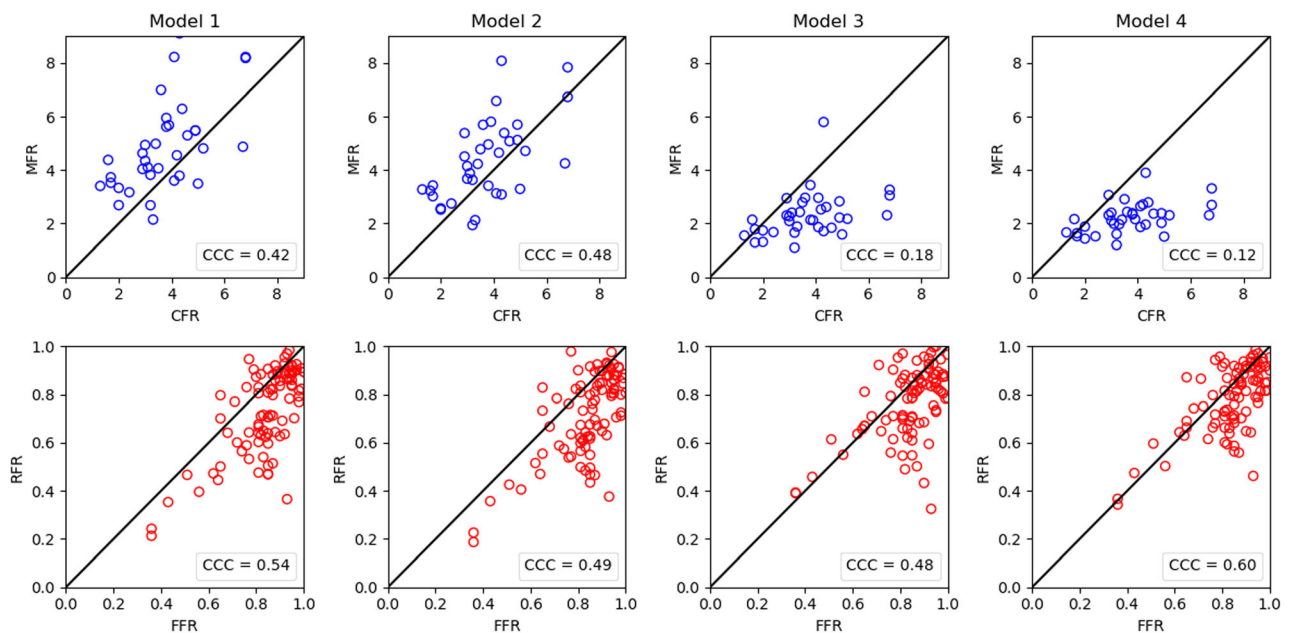

Figure 2. Plots of MFR vs CFR agreement (top row, n = 37) and of RFR vs FFR agreement (bottom row, n = 91) for each compartment model using published PS constants (Table 3) and EF computed from eqn. 3. (*PS*, the permeability and capillary surface area product; *CCC*, Concordance correlation coefficient).

compared [O-15]-water PET MBF with both Doppler flow velocity and thermodilution-derived CFR in patients referred for coronary angiography but no prior history of myocardial infarction. Using the data from their work (see Figure 6 in[30]), we computed a CCC for [O-15]-water PET MBF compared to Doppler flow velocity of 0.75 and to thermodilution of 0.49. The drop from good to moderate agreement in CCC is likely explained by several limitations in the thermodilution technique at high flows (CFR > 3) including an upward bias[7,8,30] and an increasing variance[31] compared to Doppler velocity flow.

In extraction corrected MFR in patients with a history of CAD, agreement between CFR and MFR decreases. Olsen et al.[32] studied an obese CAD population with and without prior myocardial infarctions using [Rb-82]-rubidium chloride compared to transthoracic Doppler echocardiography in the LAD territory. CCCs calculated from their work (see Figure 5 in[32]) were 0.40 in CAD patients without prior MI and 0.57 in patients with stable CAD but no prior MI history. Michelsen et al.[33] studied a cohort of 107 women (iPOWER study) with no significant obstructive CAD using [Rb-82]-rubidium chloride compared to transthoracic Doppler echocardiography of the LAD with a reported Pearson correlation of 0.36. Based on the mean and standard deviations from these groups, we estimate a bias factor of 0.39 and CCC of 0.14. IMR status was not measured in these studies and the presence of microvascular disease could lead to lower PET perfusion estimates and decreased EF corrected MFR when compared to unobstructed coronary CFR. It should be noted that the EF correction of [Rb-82]-rubidium chloride was determined from animal models,[15,34] which may introduce additional variability given the correction is larger than [N-13]-ammonia.

Fewer studies have compared invasive FFR to RFR. Stuijfzand et al.[35] studied 92 patients with CAD risk factors that included single or two-vessel disease with an overall FFR of 0.85 ± 0.14, RFR of 0.88 ±0.19 and correlation of 0.54. We compute a bias factor 0.94, which gives a CCC of 0.51. Hwang et al.[21] studied 115 patients with LAD stenosis and CAD risk factors who underwent [N-13]-ammonia PET and reported a correlation of 0.68. We estimated a bias factor of 0.74 yielding a CCC of 0.50. When comparing these prior studies, there is a trend towards better agreement between FFR vs RFR compared to CFR vs MFR, which is consistent with our findings in Table 3.

Limitations of this study include its retrospective nature and absence of an independent cohort to test the model-dependent estimates. Because agreement is based on the training dataset, it is likely overfitting exists resulting in an inflated agreement score with our

optimized model. The small sample size yielded large CCC confidence intervals, particularly for CFR vs MFR, reducing the power to detect statistical differences. PET and physiological measures were not adjusted for rate pressure product and others have found that this correction provides no improvement.[21,32,33] Although the flow measurement protocols for PET and ICA were designed to duplicate the physiological state between modalities by delivering the adenosine intravenously and at the same dose, some differences in CFR vs MFR is expected due to differences in physiological states since the measurements were not done simultaneously. It has been reported that variability of the mean transit time (used to measure CFR by thermodilution) in three consecutive measurements was 14±8% at baseline and 17±11% at hyperemia.[8] Nevertheless, Schelbert et al.[13] pointed out that the net extraction fraction derived by his experiments in open-chest dogs (and commonly used clinically) should be used with caution when applied to humans due to differences in hemodynamic states and scatter of their flow results.

NEW KNOWLEDGE GAINED

Estimation of patient-derived [N-13]-ammonia EF by maximizing the agreement between invasive and non-invasive measures of coronary and fractional flow reserve do not significantly improve PET RFR and MFR measurements over the use of traditional animal-derived EFs. Either patient-determined or traditional animal-determined EF correction, when used with the appropriate flow model, yields moderate agreement with invasive measurements of coronary flow reserve and fractional flow reserve.

CONCLUSION

The PET vs ICA moderate agreements we obtained in RFR vs FFR for all kinetic models and MFR vs CFR for two of the kinetic models are statistically similar between our patient-derived EFs and published EFs. Although we do show a trend towards improved PET vs ICA agreements in reserve measures with the newly patient-determined EFs over animal-determined EFs, we recommend that for now, time-tested kinetic models with animal-determined EFs continue to be used both for clinical and research purposes. Future enhancements to improve correlations are being pursued such as specific vessel rather than vascular territory calibration. The present results and expected improvements should facilitate our goal of predicting ICA flow measures from non-invasive PET flow studies.

Acknowledgments

Disclosures

Ernest V. Garcia, C. David Cooke, and Russell Folks receive royalties from the sale of the Emory Cardiac Toolbox and have equity positions with Syntermed, Inc. The terms of these arrangements have been reviewed and approved by Emory University in accordance with its conflict of interest policies. The remaining authors did not report any conflicts of interest.

References

1. Dilsizian V, Bacharach SL, Beanlands RS, Bergmann SR, Delbeke D, Dorbala S, et al. ASNC imaging guidelines/SNMMI procedure standard for positron emission tomography (PET) nuclear cardiology procedures. J Nucl Cardiol 2016;23:1187-1226.

2. Hutchins GD, Schwaiger M, Rosenspire KC, Krivokapich J, Schelbert H, Kuhl DE. Noninvasive quantification of regional blood flow in the human heart using N-13 ammonia and dynamic positron emission tomographic imaging. J Am Coll Cardiol 1990;15:1032-42.

3. Krivokapich J, Smith GT, Huang SC, Hoffman EJ, Ratib O, Phelps ME, et al. 13N ammonia myocardial imaging at rest and with exercise in normal volunteers: Quantification of absolute myocardial perfusion with dynamic positron emission tomography. Circulation 1989;80:1328-37.

4. A F. Uber die messung des Blutquantums in den Hertzvent rikeln. Sitzber Physik Med Ges Wurzburg. 1870;36.

5. Doucette JW, Corl PD, Payne HM, Flynn AE, Goto M, Nassi M. et al. Validation of a Doppler guide wire for intravascular measurement of coronary artery flow velocity. Circulation 1992;85:1899-1911.

6. Bach RG, Donohue TJ, Kern MJ. Intracoronary Doppler flow velocity measurements for the evaluation and treatment of coronary artery disease. Curr Opin Cardiol 1995;10:434-42.

7. Pijls NH, De Bruyne B, Smith L, Aarnoudse W, Barbato E, Bartunek J, et al. Coronary thermodilution to assess flow reserve: Validation in humans. Circulation 2002;105:2482-6.

8. Barbato E, Aarnoudse W, Aengevaeren WR, Werner G, Klauss V, Bojara W, et al. Validation of coronary flow reserve measurements by thermodilution in clinical practice. Eur Heart J 2004;25:219-23.

9. Tonino PA, De Bruyne B, Pijls NH, Siebert U, Ikeno F, van't Veer M, et al. Fractional flow reserve versus angiography for guiding percutaneous coronary intervention. N Engl J Med 2009;360:213-24.

10. Lee AK, Qutub MA, Aljizeeri A, Chow BJ. Integrating anatomical and functional imaging for the assessment of coronary artery disease. Expert Rev Cardiovasc Ther 2013;11:1301-10.

11. AlBadri A, Piccinelli M, Cho SG, Lee JM, Jaber W, De Cecco CN, et al. Rationale and design of the quantification of myocardial blood flow using dynamic PET/CTA-fused imagery (DEMYSTIFY) to determine physiological significance of specific coronary lesions. J Nucl Cardiol 2020;27:1030-9.

12. Mullani NA, Goldstein RA, Gould KL, Marani SK, Fisher DJ, O'Brien HA Jr, et al. Myocardial perfusion with rubidium-82. I. Measurement of extraction fraction and flow with external detectors. J Nucl Med 1983;24:898-906.

13. Schelbert HR, Phelps ME, Huang SC, MacDonald NS, Hansen H, Selin C, et al. N-13 ammonia as an indicator of myocardial blood flow. Circulation 1981;63:1259-72.

14. Heymann MA, Payne BD, Hoffman JI, Rudolph AM. Blood flow measurements with radionuclide-labeled particles. Prog Cardiovasc Dis. 1977;20:55-79.

15. Yoshida K, Mullani N, Gould KL. Coronary flow and flow reserve by PET simplified for clinical applications using rubidium-82 or nitrogen-13-ammonia. J Nucl Med. 1996;37:1701-12.

16. DeGrado TR, Hanson MW, Turkington TG, Delong DM, Brezinski DA, Vallee JP et al. Estimation of myocardial blood flow for longitudinal studies with 13N-labeled ammonia and positron emission tomography. J Nucl Cardiol 1996;3:494-507.

17. Scansen BA. Coronary artery anomalies in animals. Vet Sci 2017;4:20.

18. Bertho E, Gagnon G. A comparative study in three dimension of the blood supply of the normal interventricular septum in human, canine, bovine, procine, ovine and equine heart. Dis Chest 1964;46:251-62.

19. Kato T, Yasue T, Shoji Y, Shimabukuro S, Ito Y, Goto S, et al. Angiographic difference in coronary artery of man, dog, pig, and monkey. Acta Pathol Jpn 1987;37:361-73.

20. Lee JM, Kim CH, Koo BK, Hwang D, Park J, Zhang J, et al. Integrated myocardial perfusion imaging diagnostics improve detection of functionally significant coronary artery stenosis by 13N-ammonia positron emission tomography. Circ Cardiovasc Imaging 2016;9:e004768.

21. Hwang D, Jeon KH, Lee JM, Park J, Kim CH, Tong Y, et al. Diagnostic Performance of resting and hyperemic invasive physiological indices to define myocardial ischemia: Validation with (13)N-ammonia positron emission tomography. JACC Cardiovasc Interv 2017;10:751-60.

22. Lee JM, Choi KH, Hwang D, Park J, Jung JH, Kim HY, et al. Prognostic implication of thermodilution coronary flow reserve in patients undergoing fractional flow reserve measurement. JACC Cardiovasc Interv 2018;11:1423-33.

23. Piccinelli M, Cho SG, Garcia EV, Alexanderson E, Lee JM, Cooke CD, et al. Vessel-specific quantification of absolute myocardial blood flow, myocardial flow reserve and relative flow reserve by means of fused dynamic (13)NH3 PET and CCTA: Ranges in a low-risk population and abnormality criteria. J Nucl Cardiol 2020;27:1756-69.

24. Lin LI. A concordance correlation coefficient to evaluate reproducibility. Biometrics 1989;45:255-68.

25. Shrout PE, Fleiss JL. Intraclass correlations: Uses in assessing rater reliability. Psychol Bull 1979;86:420-8.

26. Carol AEN. A note on ''a concordance correlation coefficient to evaluate reproducibility.'' Biometrics 1997;53:1503-7.

27. Quinn C, Haber MJ, Pan Y. Use of the concordance correlation coefficient when examining agreement in dyadic research. Nurs Res 2009;58:368-373.

28. Lee BK, Lim HS, Fearon WF, Yong AS, Yamada R, Tanaka S, et al. Invasive evaluation of patients with angina in the absence of obstructive coronary artery disease. Circulation 2015;131:1054-60.

29. Saraste M, Koskenvuo J, Knuuti J, Toikka J, Laine H, Niemi P. et al. Coronary flow reserve: Measurement with transthoracic

Doppler echocardiography is reproducible and comparable with positron emission tomography. Clin Physiol 2001;21:114-22.

30. Everaars H, de Waard GA, Driessen RS, Danad I, van de Ven PM, Raijmakers PG, et al. Doppler flow velocity and thermodilution to assess coronary flow reserve: A head-to-head comparison with [(15)O]H2O PET. JACC Cardiovasc Interv 2018;11:2044-54.

31. Fearon WF, Farouque HM, Balsam LB, Caffarelli AD, Cooke DT, Robbins RC, et al. Comparison of coronary thermodilution and Doppler velocity for assessing coronary flow reserve. Circulation 2003;108:2198-200.

32. Olsen RH, Pedersen LR, Snoer M, Christensen TE, Ghotbi AA, Hasbak P, et al. Coronary flow velocity reserve by echocardiography: Feasibility, reproducibility and agreement with PET in overweight and obese patients with stable and revascularized coronary artery disease. Cardiovasc Ultrasound 2016;14:22.

33. Michelsen MM, Mygind ND, Pena A, Olsen RH, Christensen TE, Ghotbi AA, et al. Transthoracic Doppler echocardiography compared with positron emission tomography for assessment of coronary microvascular dysfunction: The iPOWER study. Int J Cardiol. 2017;228:435-43.

34. Lortie M, Beanlands RS, Yoshinaga K, Klein R, Dasilva JN, DeKemp RA. Quantification of myocardial blood flow with 82Rb dynamic PET imaging. Eur J Nucl Med Mol Imaging 2007;34:1765-74.

35. Stuijfzand WJ, Uusitalo V, Kero T, Danad I, Rijnierse MT, Saraste, A et al. Relative flow reserve derived from quantitative perfusion imaging may not outperform stress myocardial blood flow for identification of hemodynamically significant coronary artery disease. Circ Cardiovasc Imaging 2015;8:e002400.

Publisher's Note Springer Nature remains neutral with regard to jurisdictional claims in published maps and institutional affiliations.